# In Situ Optical Reflectance Difference Observations of CO Oxidation over Pd(100)

Onderwaater, W.G.; Taranovskyy, A.; Baarle, G.C. van; Frenken, J.W.M.; Groot, I.M.N.

THE JOURNAL OF PHYSICAL CHEMISTRY C

Article

pubs.acs.org/JPCC

# In Situ Optical Reflectance Difference Observations of CO Oxidation over Pd(100)

Willem G. Onderwaater,[†,‡] Andriy Taranovskyy,[†] Gertjan C. van Baarle,[§] Joost W. M. Frenken,[†,⊥] and Irene M. N. Groot*[,∥,†]

[†]Huygens-Kamerlingh Onnes Laboratory, Leiden University, P.O. Box 9504, 2300 RA Leiden, The Netherlands

[‡]European Synchrotron Radiation Facility, BP 220, F-38043 Grenoble Cedex 9, France

[§]Leiden Probe Microscopy B.V., J.H. Oortweg 19, 2333 CH Leiden, The Netherlands

[∥]Leiden Institute of Chemistry, Leiden University, P.O. Box 9502, 2300 RA Leiden, The Netherlands

**ABSTRACT:** Using a home-built reflectometer, we have investigated the changes in the optical reflectivity of a Pd(100) model catalyst during CO oxidation under high-pressure, high-temperature conditions. We observe changes in optical contrast when exposing the surface to CO oxidation conditions at 200 mbar from room temperature up to 400 °C. These changes in reflectivity are a result both of the formation of a surface oxide layer and of a change in surface roughness because of gas exposure. However, the reflectivity is more sensitive to the presence of a thin, flat oxide layer than to surface roughness. CO oxidation plays an important role in the decrease of the reflectivity. Since adding a reducing agent to the gas mixture renders it unlikely that the oxide thickness increases, we conclude that the observed decrease in reflectivity is dominated by increased surface roughness because of the catalytic reaction. We contribute this observed surface roughening to a Mars–van Krevelen-type reaction mechanism.

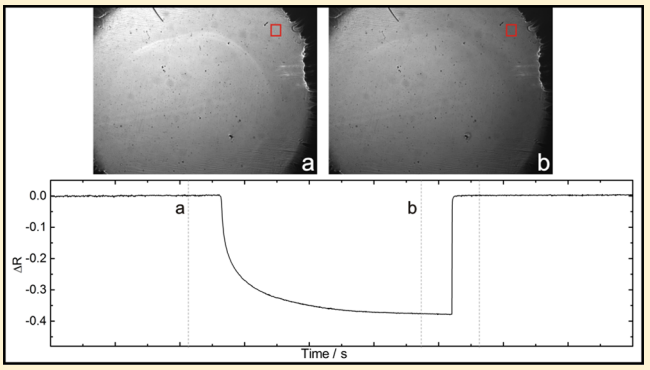


## INTRODUCTION

CO oxidation is the most widely studied chemical reaction in catalytic surface science. It has been extensively studied over metal single-crystal surfaces, such as platinum (see, e.g., refs 1−5), palladium (see, e.g., refs 6−9), ruthenium (see, e.g., refs10−14), and rhodium (see, e.g., refs 15−18). More realistic model catalysts consisting of supported nanoparticles were also used for CO oxidation studies.[15,19−26] Even though the first paper on CO oxidation was published as early as 1957,[27] novel aspects of this relatively simple reaction are still discovered frequently.

In this paper, we focus on the Pd(100) single-crystal surface. For this surface, it has been shown that a surface oxide forms during CO oxidation under (nearly) ambient conditions.[7,28−36] In high-pressure scanning tunneling microscopy (STM) studies, it was observed that the surface becomes increasingly rough when the surface oxide is formed during CO oxidation.[7] The authors explain this surface roughening as the result of a Mars–van Krevelen-type reaction mechanism,[37] in which CO from the gas phase reacts with O from the surface oxide, creating an oxygen vacancy. This vacancy will be filled with oxygen from the gas phase. When Pd atoms from the surface oxide become too poorly coordinated after reaction of CO with the surrounding surface O atoms, the Pd atoms start to diffuse, and the surface roughens. The exact structure of the surface oxide was resolved using surface X-ray diffraction (SXRD). During CO oxidation conditions under (near-)ambient pressures, the Pd(100) surface forms a $(\sqrt{5} \times \sqrt{5})R27°$ PdO(101) surface oxide.[28,31,32,36]

Spontaneous switches between the oxide and metallic phase were observed using SXRD.[28] In these studies, it was seen that the intensity of the Bragg reflection that is indicative of the oxide layer appears and disappears, showing that the surface switches between the metallic phase and the oxide phase. Because of increased surface roughening caused by the Mars–van Krevelen-type reaction mechanism, the stability of the surface oxide is lowered, and the surface will be reduced. After reduction of the surface, the roughness is removed by the fast diffusion of Pd atoms. Therefore, the oxidation and reduction of Pd(100) is accompanied by a roughening and smoothening of the surface.

We investigated this roughening and smoothening of the palladium surface in more detail using a recently developed reflectometer.[38] With this new setup, we can follow the optical changes of the surface during the catalytic reaction. In this paper, we will discuss the observed changes in the reflectivity of

**Received:** March 3, 2017
**Revised:** May 4, 2017
**Published:** May 4, 2017

  

DOI: 10.1021/acs.jpcc.7b02054
J. Phys. Chem. C 2017, 121, 11407−11415

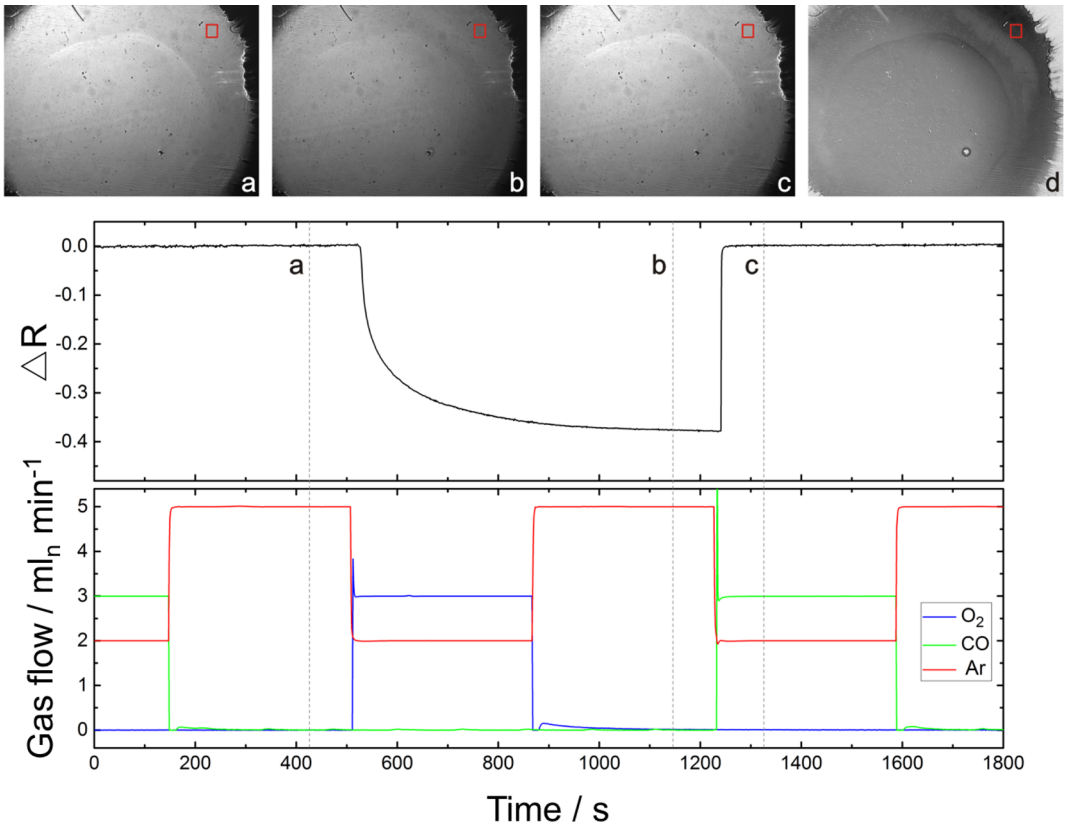


**Figure 1.** Oxidation−reduction cycles for Pd(100). The top panel shows three images (a−c) taken from the complete movie captured during oxidation−reduction cycles for Pd(100). Image a is taken during exposure to Ar + CO, image b during exposure to Ar + $O_2$, and image c again during exposure to Ar + CO. Image d shows the normalized difference $\Delta R$ between images a and b. The middle panel shows the variation of $\Delta R$ with time, averaged over the area indicated by a red rectangle in the optical images. The times of images a, b, and c are indicated by the vertical lines. The bottom panel shows the flow rates at which Ar, CO, and $O_2$ have been fed into the reactor.

the Pd(100) sample during high-pressure, high-temperature CO oxidation, presenting different models to explain it. We will show that the observed reflectivity changes are caused both by oxidation of the surface and by a change in surface roughness. Our observations correspond well with results we previously obtained using SXRD and STM.[7,28,36]

## METHODS

We measure the sample reflectance with a home-built reflectometer.[38] The sample is housed in a small flow reactor, designed by the company Leiden Probe Microscopy B.V. (LPM).[39] This minireactor is a simplified version of the ReactorSXRD chamber,[40] with the same sample mounting stage and similar reactor volume but without the UHV sample preparation environment. The chosen geometry enables a direct comparison of the optical data with the SXRD results obtained previously. With an LPM gas supply system we can set the total flow rate, total pressure (120−2000 mbar; the latter is chosen as an upper limit because of safety specifications of the reactor window), and partial pressure ratios between all constituent gases ranging from 100:1 up to 1:100. The maximum flow rate per constituent gas is 10 $mL_n$/min. With a reactor volume of ∼16 mL, the refresh rates are on the order of 1 min. This has to be taken into account when switching the gas composition in the reactor. The composition of the gas mixture that leaves the reactor is measured with a T100 high-pressure inlet residual gas analyzer of LPM.[39] The reflectometer itself consists of two stages. The presample stage starts with a light source (Thorlabs M625L3 LED with a 625 nm central wavelength). A collimator collects the light, and a spatial filter creates a parallel beam. The postsample stage collects the light, chooses a specific imaging mode, and records the result with a camera. Full details of this home-built setup are given in ref 38.

As a sample, we use a 10 mm diameter, 2 mm thick Pd(100) single crystal (Surface Preparation Laboratory). The sample in the reactor is directly mounted on a Boralectric heater, a graphite heating element embedded in boron nitride. This heater is connected to a power supply and can be heated to 800 °C, with the window of the optics part being the limiting factor. The sample holder carrying the Boralectric heater is mounted on two tantalum rods that are connected to a ceramic unit. Thermocouple wires connected to pins in the sample holder are (laser-)spot-welded on the sample to measure the temperature. The pins underneath the sample holder connect to sockets in the reactor base. The sockets are connected to feedthroughs connecting the signal to the outside of the reactor. The power supply as well as the thermocouple are computer-readable and computer-controlled. Feedback is applied between the temperature readout and heating power, in order to keep the temperature of the sample constant. Prior to all experiments, the Pd(100) sample was cleaned by reducing it in a CO atmosphere at 350 °C to ensure that the surface was in the metallic state, resulting in a highly reflective surface.



DOI: 10.1021/acs.jpcc.7b02054
J. Phys. Chem. C 2017, 121, 11407−11415

## RESULTS AND DISCUSSION

In this section we demonstrate the sensitivity of the optical reflection technique by exposing a Pd(100) surface to CO oxidation conditions at elevated temperatures and pressures. We show that even though the surface changes are very modest, a clear contrast can be observed in the optical reflection signal. We will discuss the possible origins of this observed change in reflectivity, and we will present models to explain it.

**Oxidation and Reduction.** We used the instrument described in the previous section and in ref 38 to monitor the relative reflectance difference ($\Delta R$) of a Pd(100) surface during CO oxidation. Here, we define $\Delta R = (I - I_0)/I_0$ where $I_0$ is the reflected intensity at the start of the experiment and $I$ the measured intensity at later stages of the experiment. We first investigated how the reflectance of Pd(100) changes upon oxidation and reduction of the sample (see Figure 1). The images in the top panel of Figure 1 are a direct projection of the sample on the camera. We kept the pressure constant at 200 mbar. The temperature was set at 350 °C. Small deviations from this set point were observed because of changes in heat conduction through the gas and changes in heat production by the exothermic CO oxidation reaction. We started in a gas mixture of CO and Ar, to ensure that the sample was initially in the metallic state. After this, we flushed the reactor with a flow of pure Ar. Subsequently, we introduced a mixture of $O_2$ and Ar, to oxidize the sample. Then, we flushed the reactor again with Ar, and finally, we introduced a mixture of Ar and CO, to reduce the sample again. The intermediate flushing with Ar was necessary to ensure that the previous active component, i.e., CO or $O_2$, was completely removed before the next active component was introduced.

The top panel of Figure 1 shows three optical images of the Pd(100) sample: the first during exposure to Ar and CO, the second during exposure to Ar and $O_2$, and the third again during exposure to Ar and CO. From the sequence of images, we extract a reflectivity curve with the behavior of the sample over time. We do this by integrating a small, predefined area (indicated by the red rectangle in the top panel of Figure 1) for each of the images, which results in $I(t)$. From this, we calculate $\Delta R$ (middle panel of Figure 1). The bottom panel of Figure 1 shows the flow rates of the respective gases, Ar, CO, and $O_2$. Small fluctuations in the flow rates, such as the spikes at $t$ = 430 and 1200 s, are artifacts from the gas supply system. They result from a feedback overshoot of the mass flow controllers responsible for maintaining the gas flow.

We start our experiment with the Pd(100) sample exposed to CO, which results in a surface in the metallic state. As seen from image a in Figure 1, the sample is very bright. Upon exposure to $O_2$ (image b of Figure 1), the surface becomes darker, i.e., the reflectivity decreases. From surface X-ray diffraction measurements and scanning tunneling microscopy observations, we know that the Pd(100) surface forms a thin surface oxide layer under these conditions.[7,31] After exposure to CO again, the surface returns to the metallic state as seen from the brightness of the sample (image c of Figure 1). The shape of the reflectivity curve (see middle panel of Figure 1) shows a rapid initial decrease when changing the CO flow to an $O_2$ flow. Over time, this decrease in reflectivity gradually approaches a plateau value. From the analysis of the full time sequence of optical images, we observe that the decrease in reflectivity upon introduction of oxygen in the reactor starts closest to the reactor inlet. The same is observed for the reduction after introducing CO in the reactor.

*Contrast Mechanism.* The images in Figure 1 show that the optical properties of the sample change upon exposure to different gases. With our setup, we are able to follow the change in reflectivity over the entire surface while exposing the sample to varying catalytic conditions. Various physical processes can cause a decrease in the reflectivity. The oxidation of the palladium increases its roughness, both for the top surface and for the oxide−metal interface. Additionally, the optical properties of the palladium oxide and of the metallic palladium are different, which also causes a change in reflectivity of the surface. From these images, we cannot conclude which of these two effects is the cause of the change in reflectivity, accompanying the $O_2$-induced oxidation of Pd(100). Understanding the contrast mechanism will help us to understand the surface dynamics, by examining how the reflectivity changes on different locations on the sample correlate.

If the contrast results from the formation of the palladium oxide, we expect $\Delta R$ to initially decrease quickly. The Mott−Cabrera theory for oxide growth on metals[41] predicts a decreasing growth rate by an increasing limitation of the diffusion of oxygen atoms from the surface through the thin oxide layer. Therefore, we expect the growth rate to obey $\Delta R \propto -[\ln(t)]^{2/3}$. However, if the contrast results from the generation of roughness, we expect it to follow $\Delta R \propto -\sqrt{\ln(t)}$.[42] The observed time dependence of the change in $\Delta R$ after oxidation does not favor either of these two models. Although the $O_2$ partial pressure is identical everywhere, we see two regions with different responses (image d in Figure 1). In the top-left corner, the reflectivity decreases less than that in other areas of the surface. This suggests that the growth of the palladium oxide depends either on initial conditions of the surface or on other growth parameters. We now address the question regarding the origin of the contrast mechanism by calculating the effects of both surface roughening and oxide formation on the reflectivity separately.

To estimate the effect of the oxide layer on the reflectivity, we consider a thin palladium oxide film on top of a smooth Pd surface. The change in reflectivity is then caused by a difference in the refractive index of palladium oxide with respect to palladium. We calculate the Fresnel coefficient for reflection on a single layer using the following.[43]

$$R = \left| \frac{r_{01} + r_{12} e^{2i\beta}}{1 + r_{01} r_{12} e^{2i\beta}} \right|^2$$

Here, the individual Fresnel components $r_{ij}$'s for light under normal incidence are given by

$$r_{ij} = \frac{n_i - n_j}{n_i + n_j}$$

with $n_i$ the (complex) refractive index of layer $i$. In this notation, the index 0 indicates the ambient gas environment, 1 the palladium oxide layer, and 2 the bulk palladium. $\beta$ describes the phase change of the light in the thin film with thickness $d$. Under normal incidence, this corresponds to $\beta = \frac{2\pi n_1 d}{\lambda}$. If we assume the refractive index of the thin layer is that of the palladium bulk oxide (PdO), we can calculate the change in reflection coefficient as a function of the layer thickness.[44] The result is shown in Figure 2. The left panel of Figure 2 shows the



DOI: 10.1021/acs.jpcc.7b02054
J. Phys. Chem. C 2017, 121, 11407−11415

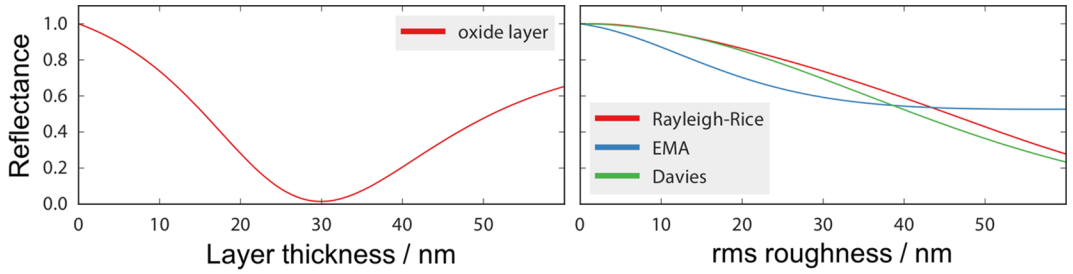


**Figure 2.** Reflected intensity for a surface oxide layer (left panel) and for three roughness models (right panel). The reflected intensity is normalized by the reflectance of a bare, smooth palladium surface of 0.71. The formation of a thin oxide layer is a more dominant factor for the decrease in reflectance than the introduction of roughness. To compare the decrease in calculated intensity with the EMA model with the Davies and the Rayleigh–Rice models, we approximate the layer thickness to be 3 times the root-mean-square roughness.

reflected intensity for a surface oxide layer as a function of oxide layer thickness. The right panel shows the reflected intensity for a surface oxide layer as a function of its root-mean-square roughness for three different roughness models: the Rayleigh–Rice model,[45] the effective medium approximation, and the model from Davies.[46] These models will be described in detail below. Only a thin layer (~10 nm) is needed at this wavelength to achieve the observed decrease in the reflectivity. Almost complete absorption is calculated to happen around 30 nm. The remarkable sensitivity of the reflected intensity to the oxide thickness occurs because of destructive interference of light reflected from the gas-to-oxide interface with light reflected from the oxide-to-metal interface below. The near-extinction of the reflected intensity around 30 nm thickness indicates that the amplitude of the light reflecting from the gas-to-oxide interface is almost equal to the amplitude of light reflecting from the oxide-to-metal interface.

Next, we will investigate the expected effect of the roughness on $\Delta R$. The response of a rough surface to incoming specular light has been investigated extensively over the last 60 years. We recognize three categories of approaches, depending on the in-plane correlation length of the surface roughness. First, when the in-plane correlation length is large with respect to the wavelength of the employed light, the diffuse reflection of the light can be described with the Fresnel coefficients on the local slopes of the surface. This gives the response a geometrical character, where the angles of reflection with respect to the incoming beam can be obtained from the distribution of slopes. This decreases the specular reflectance and increases the reflection in the off-specular directions.[47]

Second, when the characteristic length scale of the roughness is on the order of the wavelength, a Rayleigh scattering approach becomes more appropriate. Also in this case, roughness leads to an increase in off-specular scattering and a decrease in specular scattering. Third, when the correlation length is much smaller than the wavelength, no off-specular scattering is observed, but still, the reflectance decreases.[48] The lost intensity is transmitted through the surface and absorbed. In this regime, the roughness can be estimated with the effective medium approximation (EMA) by replacing the roughness with a thin film with a dielectric constant that is an average of the dielectric constants of the ambient and the reflecting medium. Since roughness growth models[42] predict that the characteristic in-plane length scale starts small and increases over time, we expect to progress through these three regimes in reverse order.

We calculate the effective dielectric constant in the EMA by assuming that the layer consists of a random mixture of the oxygen-gas atmosphere and substrate material. The effective refractive index $n_{\mathrm{EMA}}$ is given by

$$v_0\frac{{n_0}^2 - {n_{\mathrm{EMA}}}^2}{{n_0}^2 + 2{n_{\mathrm{EMA}}}^2} + v_1\frac{{n_1}^2 - {n_{\mathrm{EMA}}}^2}{{n_1}^2 - 2{n_{\mathrm{EMA}}}^2} = 0$$

Here $n_0$ and $n_1$ are the refractive indices of oxygen and of the substrate, respectively. $v_0$ and $v_1$ are the volume fractions of oxygen and substrate material in the mixture, respectively, which we choose to both be 0.5.[49] The reflectivity can then be calculated using the method described above for the palladium oxide layer. Using this EMA approach, we find that a mixed layer with a thickness of ~35 nm would be required to explain the measured reduction in reflected intensity upon exposure of the surface to $O_2$. This corresponds to a short-wavelength roughness with a valley-to-top amplitude of 35 nm.

In the intermediate regime, where the correlation length of the surface is of the order of the wavelength, we estimate the roughness using the Rayleigh–Rice formalism. Here, we have followed the procedure described in ref 45. The change in the Fresnel coefficient under normal incidence can be calculated using

$$\Delta r_{p,s} = \iint f_{p,s}(q_x, q_y)\, S(q_x, q_y)\, \mathrm{d}q_x\, \mathrm{d}q_y$$

Here, $q_x$ and $q_y$ are the in-plane momentum transfer components of the diffracted wave; $S(q_x, q_y)$ is the spectral density function of the surface roughness, and $f_{p,s}(q_x, q_y)$ stands for the optical response for polarizations $s$ and $p$, which are identical to each other for the case of normal incidence on an isotropic surface. We estimate the spectral density function of the surface roughness to be

$$S(q) = \frac{\alpha w^2 \xi^2}{\pi}\frac{1}{(1 + \xi^2 q^2)^{\alpha+1}}$$

with $w$ the root-mean-square roughness, $\xi$ the correlation length, and $\alpha$ the Hurst exponent. The Hurst exponent defines the scaling relation between the roughness and the lateral length scale: $\langle[h(d + r) - h(d)]^2\rangle = cr^{\alpha}$, where $h(d)$ is the height function and $c$ a constant. We use $\alpha = 0.7$ and set $\xi$ equal to the root-mean-square roughness $w$. This approach predicts a root-mean-square roughness of 30 nm for the observed decrease in $\Delta R$.

The estimated effect of the surface roughness when the wavelength is much smaller than the characteristic in-plane length scale was calculated by Davies using

$$R_s = R_0 \mathrm{e}^{-\left(\frac{4\pi w}{\lambda}\right)^2}$$



DOI: 10.1021/acs.jpcc.7b02054
J. Phys. Chem. C 2017, 121, 11407–11415

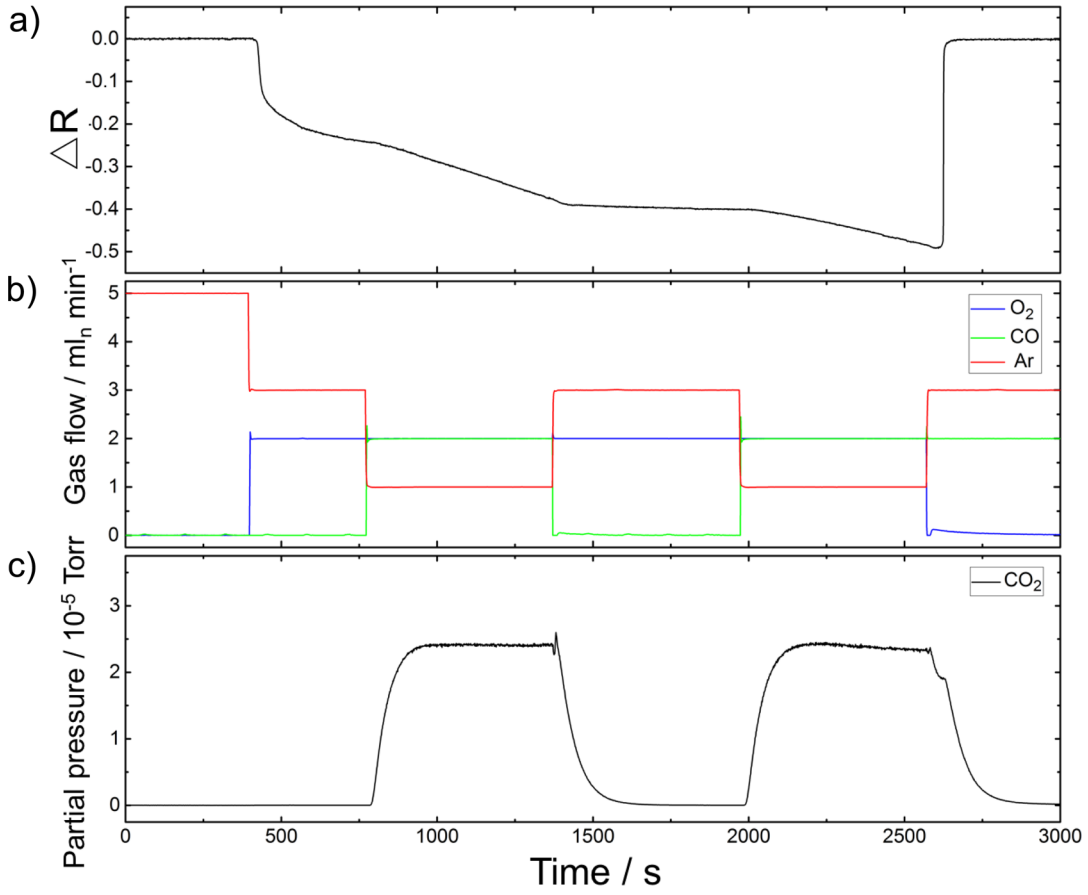


**Figure 3.** CO oxidation on Pd(100). (a) Variation of $\Delta R$ with time, averaged over the same sample area as indicated in Figure 1. (b) Flow rates at which Ar, CO, and $O_2$ have been fed into the reactor. (c) Production of $CO_2$ as measured with the T100 residual gas analyzer.

where $R_0$ is the reflection coefficient of a smooth surface, $w$ the root-mean-square height variation, and $\lambda$ the wavelength.[46] This approximation assumes that the root-mean-square roughness is small compared to the wavelength, and that both the height distribution and the autocorrelation function are Gaussian-distributed. Using this approximation, we find that a roughness value of $w$ = 28 nm is required to fit the experimentally observed reduction in reflectivity.

Although all described roughness estimates are only applicable in their own respective regimes, they indicate a significantly higher sensitivity of the reflectivity to the presence of a thin flat oxide layer than to surface roughness. This suggests that, whatever lateral length scale is characteristic for the surface roughness, we should expect $\Delta R$ to be dominated by the formation of an oxide at the surface. The oxide thickness estimated on the basis of the measured $\Delta R$ is somewhat higher than the oxide thickness of 4 nm that was determined previously with SXRD.[31] However, that oxide was grown under different reaction conditions, and its thickness might be underestimated.

So far, we have considered the separate contributions to $\Delta R$ of the presence of an oxidized surface layer and of surface roughness. When the surface is both oxidized and rough, the two effects on the reflectivity should be summed. An additional effect, involving the excitation of surface plasmons,[50] is possible, when the roughness obeys certain conditions. The characteristics of surface plasmons are highly sensitive to the dielectric properties of the interface as they are purely a surface effect. This renders the reflection coefficient also sensitive to a combination of interface roughness and oxide thickness.

**CO Oxidation.** *CO Oxidation at Constant Temperature.* To further differentiate between oxidation and surface roughening as the main cause for the observed decrease in reflectivity, we investigated CO oxidation at a constant temperature of 350 °C (see Figure 3). Again, we started the experiment with a reduced Pd sample in the metallic state ($t$ = 0−394 s). We oxidized this surface in a mixture of $O_2$ and Ar ($t$ = 394−768 s). Subsequently, we lowered the Ar flow rate and increased the CO flow rate from zero to the same value as the $O_2$ flow rate, to study CO oxidation ($t$ = 768−1396 s). The CO oxidation reaction was confirmed by the observation of the $CO_2$ signal in the gas analyzer. After 601 s ($t$ = 1396 s), we interrupted the CO oxidation reaction by flowing a mixture of $O_2$ and Ar for 601 s ($t$ = 1396−1970 s). Afterward, we restarted the reaction by reducing the Ar flow and adding CO to the gas mixture ($t$ = 1970−2571 s). Subsequently, $O_2$ was removed until the Pd surface was fully reduced ($t$ = 2571−3000 s). Figure 3 shows the results of this experiment.

When comparing the results of CO oxidation versus pure oxidation, we observe clear differences. When the Pd(100) surface is oxidized in a mixture of oxygen and argon, the reflectivity signal (Figure 3a) reaches a plateau value. When the CO oxidation reaction is taking place, the reflectivity starts decreasing again. When we stop the CO oxidation reaction and expose the surface to a mixture of Ar and $O_2$, we do not observe a further decrease in reflectivity, but instead, $\Delta R$ remains


DOI: 10.1021/acs.jpcc.7b02054
J. Phys. Chem. C 2017, 121, 11407−11415

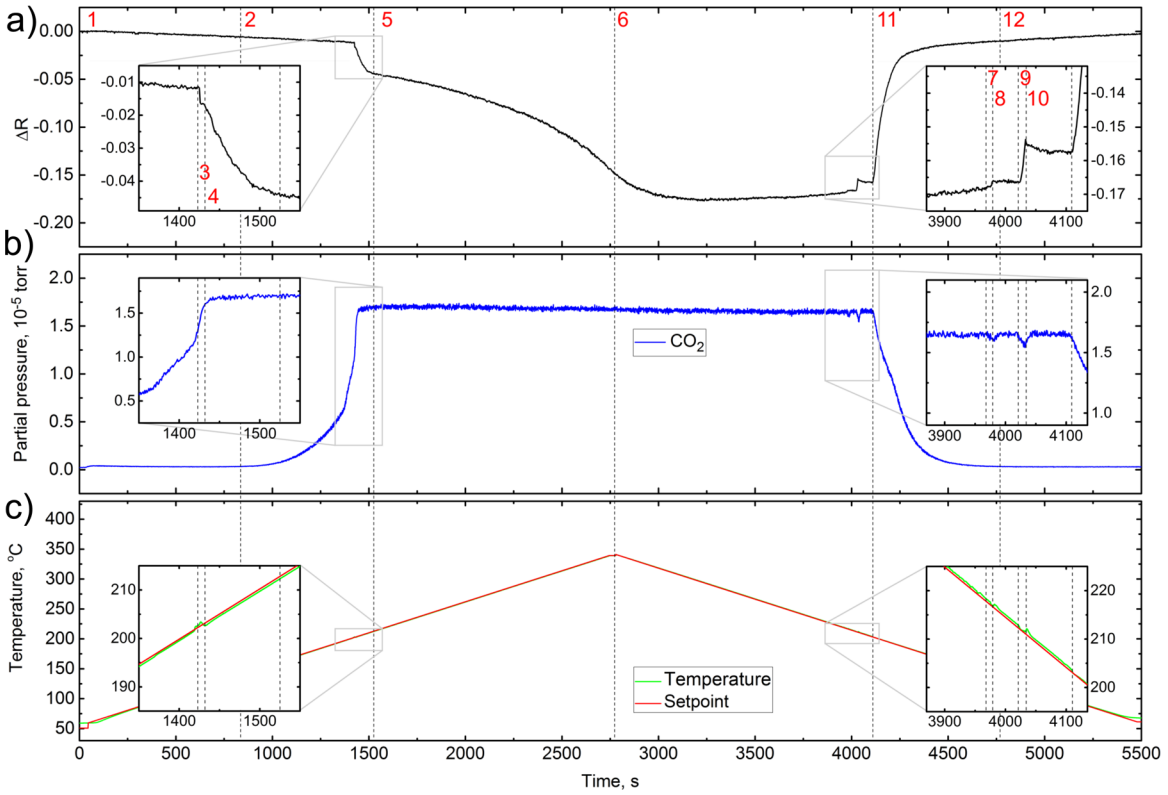


**Figure 4.** CO oxidation on Pd(100) during large temperature variations. (a) Variation of $\Delta R$ with time, averaged over the same sample area as indicated in Figure 1. (b) Production of $CO_2$ as measured with the T100 residual gas analyzer. (c) Set-point temperature and actual sample temperature. The different episodes indicated are discussed in the main text. The insets show enlarged views of two episodes of interest with rapid changes in reactivity and reflectance.

unaffected. It starts decreasing again when we resume the CO oxidation reaction.

It is clear that the CO oxidation reaction plays an important role in the decrease of the reflectivity. Since it is unlikely that the addition of a reducing agent to the gas mixture increases the oxide thickness, we interpret the observed decrease in reflectivity as a strong indication that surface roughness is responsible for this. This is fully consistent with our observations of SXRD and STM.[7,31] During the CO oxidation reaction, the surface of the oxide layer becomes rough, as observed by STM,[7] while SXRD shows that the oxide−metal interface becomes increasingly rough during reaction.[31]

A second experimental indication that roughness is the cause of contrast can be seen at $t$ = 2571 s in Figure 3, where the surface is reduced after a period of CO oxidation. After CO oxidation, the recovery of the surface that starts at $t$ = 2571 s and makes the surface return to the initial, zero value of $\Delta R$ takes as long as 80 s. This should be compared to the much shorter recovery time of 4 s found in Figure 1 at 1220 s after exposure of the surface to pure $O_2$. Whereas the reduction is a rapid, chemical process, the smoothening of the surface requires the lateral diffusion of large numbers of Pd atoms over large distances, which makes this a slow process, hence the relatively slow recovery.

Although not all regions of the surface vary equally strongly in reflectivity, the qualitative behavior of the entire surface is uniform and completely synchronous. This suggests that the entire oxidized surface is participating in the CO oxidation reaction. If the oxidized area were completely insensitive to the presence of CO, the reflectivity of these areas would not change during the reaction. Furthermore, if the presence of CO were to lead to a local reduction of the surface, this would lead either to a decrease in the thickness of the oxide, or even to the complete local removal of the oxide and the ensuing smoothening of the surface. In both cases, we should expect the reflectivity to stay constant or increase, as opposed to the observed steady decrease.

The origin of surface roughness has been debated previously. Assuming the reaction follows a Langmuir−Hinshelwood-type mechanism, the roughness generation for Pt(110) has been explained by invoking mass transport via restructuring of the surface during switches from CO-covered to $O_2$-covered.[51] However, this explanation has gained no further support after the discovery of a thin oxide layer present during the roughening phase.[1,5] Then, it was proposed that a Mars−van Krevelen-type mechanism causes the surface to roughen. In this reaction, CO molecules react with O atoms in the surface oxide to form $CO_2$. The oxygen vacancy, left behind in the surface oxide, is then quickly filled up by oxygen from the gas phase. In the case that a rapid succession of local CO oxidation events leads to a temporary, strong, local reduction of the surface oxide, for example, in the form of the simultaneous absence of 3 O atoms, a Pd atom near the multiple-oxygen vacancy may become so loosely bound that it can liberate itself from the oxide matrix and diffuse over the oxide surface. After a brief journey, such a diffusing metal atom will be reoxidized on top of the oxide. The net effect of this relocation is a local depression at the original location of the metal atom and a new protrusion at its new location, which indeed adds to the roughness of the surface. Our observation of a steady reduction



DOI: 10.1021/acs.jpcc.7b02054
J. Phys. Chem. C 2017, 121, 11407−11415

in reflectivity during CO oxidation on the oxidized Pd(100) surface is fully consistent with this steady reaction-induced roughening and thus supports the Mars–van Krevelen hypothesis.

*CO Oxidation During Large Temperature Variations.* A second way to explore the dependence of the CO oxidation reaction mechanism on the reaction conditions is illustrated in Figure 4, where the temperature is ramped up and down linearly from room temperature to 300 °C and back. During this process, the gas mixture in the reactor is kept constant at a total pressure of 200 mbar, an $O_2$ flow rate of 3 $mL_n$/min, and a CO flow rate of 1.5 $mL_n$/min. We analyzed the composition of the gas exhaust to monitor the $CO_2$ production. Panel a of Figure 4 shows the behavior of the surface reflectivity, averaged over a small part of the surface, similar to the rectangle indicated in the images of Figure 1.

In the episode labeled 1 in Figure 4, we start at low temperature. The increase in temperature is initially accompanied by a modest, slow decrease of $\Delta R$, which can be ascribed to thermally induced drift of the Pd sample. In episode 2, we see an increase of the $CO_2$ production. In episode 3, the $CO_2$ production shows a sharp increase. Coinciding with this chemical change in episode 2, $\Delta R$ shows a sudden, small decrease of 0.5%. The resulting $\Delta R$ is maintained for only a few seconds, until episode 4 starts, in which the partial pressure of $CO_2$ remains constant, but $\Delta R$ decreases rapidly with time. The start of episode 5 marks the point in time where the reduction of $\Delta R$ slows down significantly. In this episode, the composition of the gas that leaves the reactor is constant. Episode 6 starts at the point in time when we have reached the maximum temperature and start cooling. Initially, the reduction of $\Delta R$ slows down, and $\Delta R$ levels off. In the second half of episode 6, $\Delta R$ increases somewhat. In episode 7, we see the combination of a temporary decrease in $CO_2$ production and a very small upward step in $\Delta R$, while in episode 8 the $CO_2$ production rate is at its previous level. This cycle repeats itself at episodes 9 and 10, this time with a more pronounced increase in $\Delta R$. In episode 11, the $CO_2$ production severely decreases. This coincides with an almost full recovery of the reflectivity. In the final episode, 12, the measured $CO_2$ partial pressure falls in the noise level. The slow increase in reflected intensity results from the reverse thermal drift of that experienced in episode 1.

Armed with only the $\Delta R$ and gas composition information in Figure 4, it is impossible to give a full description of all changes in surface structure and reaction mechanisms during the experiment. In our interpretation, we make use of previous experiments on Pd(100), performed under comparable conditions, with other structurally sensitive techniques, in particular STM and SXRD.[7,28,31,32,36] This brings us to the following scenario. In episode 1, the sample is CO-poisoned and therefore in a metallic state. The $CO_2$ production follows the Langmuir–Hinshelwood mechanism. As the temperature increases, the surface is increasingly populated by O atoms. We speculate that, in the last part of episode 2, the reaction rate increases as a result of the presence of an alternative and more reactive coadsorption structure of O and CO on the metal surface. We interpret the sudden decrease of $\Delta R$, accompanied by the jump in $CO_2$ partial pressure, as the consequence of the sudden formation of a surface oxide, as has been identified in SXRD and STM experiments.[7,31] This surface oxide forms the starting point for the rapid growth of a thin film of a few-nanometers-thick bulk-like PdO. This goes hand-in-hand with the buildup of additional roughness and, hence, a further reduction of $\Delta R$ (episode 4). This growth of the bulk-like oxide is self-terminating, and therefore, the rapid reduction of $\Delta R$ also comes to an end (episode 5). Under these conditions, the reaction proceeds according to the Mars–van Krevelen mechanism. As we have seen before, this reaction mechanism leads to a steady roughening of the surface and the corresponding steady reduction of $\Delta R$. When the temperature is decreased again in episode 6, the reaction rate, which is mostly limited by the diffusion of CO in the gas phase, slows down. This progressively reduces the rate at which $\Delta R$ drops. We interpret the effects in episodes 7–10 as reduction and oxidation cycles, induced by the interplay of the decreasing temperature and the changes in surface roughness. In episode 11, the surface is fully reduced. With the removal of the rough oxide, the diffusivity of the palladium atoms is increased, and the surface smoothens. In the gas analysis, we can see that, upon reduction of the surface, the reactivity is decreased. The reaction is back to the initial Langmuir–Hinshelwood mechanism.

## CONCLUSIONS

We have presented the first results on in situ reflectance difference observations on CO oxidation over Pd(100) under high-pressure, high-temperature conditions. With this method, we are able to follow the optical response of a model catalyst surface to the exposure to CO and $O_2$ over a broad temperature range. We investigate the observed change in reflectivity of the surface upon exposure to CO oxidation conditions using two possible origins: the formation of an (surface) oxide and changes in the roughness of the surface. From this modeling, we conclude that the change in reflectivity is caused both by oxidation of the surface and by a change in roughness. However, the reflectivity is more sensitive to the presence of a thin flat oxide layer than to surface roughness. From the measured change in reflectivity and the modeling of $\Delta R$, we estimate an oxide layer thickness that is slightly higher than the layer thickness determined with SXRD.

When comparing the results of separate oxidation–reduction cycles to the results of CO oxidation (both at constant temperature and during a temperature ramp), it is clear that CO oxidation plays an important role in the decrease of the reflectivity. Since adding a reducing agent to the gas mixture renders it unlikely that the oxide thickness increases, we conclude that the observed decrease in reflectivity is dominated by increased surface roughness because of the catalytic reaction. This increased surface roughness has been observed before by STM and SXRD. We contribute this observed surface roughening to a Mars–van Krevelen-type reaction mechanism.

## AUTHOR INFORMATION

### Corresponding Author

*E-mail: i.m.n.groot@lic.leidenuniv.nl. Phone: +31 71 5277361.

### ORCID

Irene M. N. Groot: 0000-0001-9747-3522

### Present Address

⊥J.W.M.F.: Advanced Research Center for Nanolithography, P.O. Box 93019, 1090 BA Amsterdam, The Netherlands.

### Notes

The authors declare no competing financial interest.



DOI: 10.1021/acs.jpcc.7b02054
J. Phys. Chem. C 2017, 121, 11407–11415

## ■ ACKNOWLEDGMENTS

This work was financially supported through Grant 12825 of Stichting Technologische Wetenschappen (STW) of The Netherlands Organization for Scientific Research (NWO). I.M.N.G. acknowledges support through a Veni grant of STW. The authors thank Michiel de Dood (Leiden Institute of Physics) for fruitful discussions.

## ■ REFERENCES

(1) Ackermann, M. D.; Pedersen, T. M.; Hendriksen, B. L. M.; Robach, O.; Bobaru, S. C.; Popa, I.; Quiros, C.; Kim, H.; Hammer, B.; Ferrer, S.; et al. Structure and reactivity of surface oxides on Pt(110) during catalytic CO oxidation. *Phys. Rev. Lett.* **2005**, *95*, 255505.

(2) Balmes, O.; Prevot, G.; Torrelles, X.; Lundgren, E.; Ferrer, S. Diatomic steps in Pt(997) surfaces are better catalysts than monatomic steps for the CO oxidation reaction near atmospheric pressure. *ACS Catal.* **2016**, *6*, 1285−1291.

(3) Krick Calderón, S.; Grabau, M.; Óvári, L.; Kress, B.; Steinrück, H.-P.; Papp, C. CO oxidation on Pt(111) at near ambient pressures. *J. Chem. Phys.* **2016**, *144*, 044706.

(4) Gao, F.; Wang, Y.; Cai, Y.; Goodman, D. W. CO oxidation on Pt-group metals from ultrahigh vacuum to near atmospheric pressures. 2. Palladium and platinum. *J. Phys. Chem. C* **2009**, *113*, 174−181.

(5) Hendriksen, B. L. M.; Frenken, J. W. M. CO oxidation on Pt(110): Scanning tunneling microscopy inside a high-pressure flow reactor. *Phys. Rev. Lett.* **2002**, *89*, 046101.

(6) Blomberg, S.; Zetterberg, J.; Gustafson, J.; Zhou, J.; Brackmann, C.; Lundgren, E. Comparison of AP-XPS and PLIF measurements during CO oxidation over Pd single crystals. *Top. Catal.* **2016**, *59*, 478−486.

(7) Hendriksen, B. L. M.; Bobaru, S. C.; Frenken, J. W. M. Oscillatory CO oxidation on Pd(100) studied with in situ scanning tunneling microscopy. *Surf. Sci.* **2004**, *552*, 229−242.

(8) Kaichev, V. V.; Prosvirin, I. P.; Bukhtiyarov, V. I.; Unterhalt, H.; Rupprechter, G.; Freund, H.-J. High-pressure studies of CO adsorption on Pd(111) by X-ray photoelectron spectroscopy and sum-frequency generation. *J. Phys. Chem. B* **2003**, *107*, 3522−3527.

(9) Nakao, K.; Ito, S.-i.; Tomishige, K.; Kunimori, K. Structure of activated complex of CO2 formation in a CO + O2 reaction on Pd(110) and Pd(111). *J. Phys. Chem. B* **2005**, *109*, 17553−17559.

(10) Over, H.; Kim, Y. D.; Seitsonen, A. P.; Wendt, S.; Lundgren, E.; Schmid, M.; Varga, P.; Morgante, A.; Ertl, G. Atomic-scale structure and catalytic reactivity of the RuO2(110) surface. *Science* **2000**, *287*, 1474−1476.

(11) Over, H.; Balmes, O.; Lundgren, E. Direct comparison of the reactivity of the non-oxidic phase of Ru(0 0 0 1) and the RuO2 phase in the CO oxidation reaction. *Surf. Sci.* **2009**, *603*, 298−303.

(12) Gao, F.; Wang, Y.; Cai, Y.; Goodman, D. W. CO oxidation over Ru(0 0 0 1) at near-atmospheric pressures: From chemisorbed oxygen to RuO2. *Surf. Sci.* **2009**, *603*, 1126−1134.

(13) Gao, F.; Goodman, D. W. CO oxidation over ruthenium: identification of the catalytically active phases at near-atmospheric pressures. *Phys. Chem. Chem. Phys.* **2012**, *14*, 6688−6697.

(14) He, Y. B.; Knapp, M.; Lundgren, E.; Over, H. Ru(0001) model catalyst under oxidizing and reducing reaction conditions: In situ high-pressure surface X-ray diffraction study. *J. Phys. Chem. B* **2005**, *109*, 21825−21830.

(15) Blomberg, S.; Westerström, R.; Martin, N.; Lundgren, E.; Andersen, J.; Messing, M.; Gustafson, J. A high pressure X-ray photoelectron spectroscopy study of oxidation and reduction of Rh(100) and Rh nanoparticles. *Surf. Sci.* **2014**, *628*, 153−158.

(16) Gustafson, J.; Westerström, R.; Balmes, O.; Resta, A.; van Rijn, R.; Torrelles, X.; Herbschleb, C.; Frenken, J. W. M.; Lundgren, E. Catalytic activity of the Rh surface oxide: CO oxidation over Rh(111) under realistic conditions. *J. Phys. Chem. C* **2010**, *114*, 4580−4583.

(17) Gustafson, J.; Blomberg, S.; Martin, N. M.; Fernandes, V.; Borg, A.; Liu, Z.; Chang, R.; Lundgren, E. A high pressure x-ray photoelectron spectroscopy study of CO oxidation over Rh(100). *J. Phys.: Condens. Matter* **2014**, *26*, 055003.

(18) Zhang, C.; Lundgren, E.; Carlsson, P.-A.; Balmes, O.; Hellman, A.; Merte, L. R.; Shipilin, M.; Onderwaater, W.; Gustafson, J. Faceting of rhodium(553) in realistic reaction mixtures of carbon monoxide and oxygen. *J. Phys. Chem. C* **2015**, *119*, 11646−11652.

(19) Assmann, J.; Narkhede, V.; Khodeir, L.; Löffler, E.; Hinrichsen, O.; Birkner, A.; Over, H.; Muhler, M. On the nature of the active state of supported ruthenium catalysts used for the oxidation of carbon monoxide: Steady-state and transient kinetics combined with in situ infrared spectroscopy. *J. Phys. Chem. B* **2004**, *108*, 14634−14642.

(20) Dellwig, T.; Hartmann, J.; Libuda, J.; Meusel, I.; Rupprechter, G.; Unterhalt, H.; Freund, H.-J. Complex model catalysts under UHV and high pressure conditions: CO adsorption and oxidation on alumina-supported Pd particles. *J. Mol. Catal. A: Chem.* **2000**, *162*, 51−66. In honor of Prof. H. Knozinger on the occasion of his 65th birthday.

(21) Gao, F.; Wang, Y.; Goodman, D. W. Reaction kinetics and polarization-modulation infrared reflection absorption spectroscopy (PM-IRAS) investigation of CO oxidation over supported Pd-Au alloy catalysts. *J. Phys. Chem. C* **2010**, *114*, 4036−4043.

(22) Grass, M.; Zhang, Y.; Butcher, D.; Park, J.; Li, Y.; Bluhm, H.; Bratlie, K.; Zhang, T.; Somorjai, G. A. A reactive oxide overlayer on rhodium nanoparticles during CO oxidation and its size dependence studied by in situ ambient-pressure X-ray photoelectron spectroscopy. *Angew. Chem., Int. Ed.* **2008**, *47*, 8893−8896.

(23) Hejral, U.; Vlad, A.; Nolte, P.; Stierle, A. In situ oxidation study of Pt nanoparticles on MgO(001). *J. Phys. Chem. C* **2013**, *117*, 19955−19966.

(24) Kasper, N.; Stierle, A.; Nolte, P.; Jin-Phillipp, Y.; Wagner, T.; de Oteyza, D.; Dosch, H. In situ oxidation study of MgO(100) supported Pd nanoparticles. *Surf. Sci.* **2006**, *600*, 2860−2867.

(25) McClure, S. M.; Lundwall, M.; Yang, F.; Zhou, Z.; Goodman, D. W. Characterization of active sites on Rh/SiO2 model catalysts. *J. Phys.: Condens. Matter* **2009**, *21*, 474223.

(26) Muller, P.; Hejral, U.; Rutt, U.; Stierle, A. In situ oxidation study of Pd-Rh nanoparticles on MgAl2O4(001). *Phys. Chem. Chem. Phys.* **2014**, *16*, 13866−13874.

(27) Eischens, R. P.; Pliskin, W. A. Infrared Study of the Catalyzed Oxidation of CO. *Adv. Catal.* **1957**, *9*, 662−668.

(28) Hendriksen, B. L. M.; Ackermann, M. D.; van Rijn, R.; Stoltz, D.; Popa, I.; Balmes, O.; Resta, A.; Wermeille, D.; Felici, R.; Ferrer, S.; et al. The role of steps in surface catalysis and reaction oscillations. *Nat. Chem.* **2010**, *2*, 730−734.

(29) Fernandes, V.; Gustafson, J.; Svenum, I.-H.; Farstad, M.; Walle, L.; Blomberg, S.; Lundgren, E.; Borg, A. Reduction behavior of oxidized Pd(100) and Pd75Ag25(100) surfaces using CO. *Surf. Sci.* **2014**, *621*, 31−39.

(30) Kondoh, H.; Toyoshima, R.; Monya, Y.; Yoshida, M.; Mase, K.; Amemiya, K.; Mun, B. S. In situ analysis of catalytically active Pd surfaces for CO oxidation with near ambient pressure XPS. *Catal. Today* **2016**, *260*, 14−20. Surface Analysis and Dynamics (SAND).

(31) Lundgren, E.; Gustafson, J.; Mikkelsen, A.; Andersen, J. N.; Stierle, A.; Dosch, H.; Todorova, M.; Rogal, J.; Reuter, K.; Scheffler, M. Kinetic hindrance during the initial oxidation of Pd(100) at ambient pressures. *Phys. Rev. Lett.* **2004**, *92*, 046101.

(32) Gustafson, J.; Shipilin, M.; Zhang, C.; Stierle, A.; Hejral, U.; Ruett, U.; Gutowski, O.; Carlsson, P. A.; Skoglundh, M.; Lundgren, E. High-energy surface X-ray diffraction for fast surface structure determination. *Science* **2014**, *343*, 758−761.

(33) Shipilin, M.; Hejral, U.; Lundgren, E.; Merte, L. R.; Zhang, C.; Stierle, A.; Ruett, U.; Gutowski, O.; Skoglundh, M.; Carlsson, P.-A.; et al. Quantitative surface structure determination using in situ high-energy SXRD: Surface oxide formation on Pd(100) during catalytic CO oxidation. *Surf. Sci.* **2014**, *630*, 229−235.

(34) Shipilin, M.; Gustafson, J.; Zhang, C.; Merte, L. R.; Stierle, A.; Hejral, U.; Ruett, U.; Gutowski, O.; Skoglundh, M.; Carlsson, P.-A.; et al. Transient structures of PdO during CO oxidation over Pd(100). *J. Phys. Chem. C* **2015**, *119*, 15469−15476.



DOI: 10.1021/acs.jpcc.7b02054
*J. Phys. Chem. C* 2017, 121, 11407−11415

(35) Toyoshima, R.; Yoshida, M.; Monya, Y.; Suzuki, K.; Mun, B. S.; Amemiya, K.; Mase, K.; Kondoh, H. Active surface oxygen for catalytic CO oxidation on Pd(100) proceeding under near ambient pressure conditions. *J. Phys. Chem. Lett.* **2012**, *3*, 3182−3187.
(36) van Rijn, R.; Balmes, O.; Resta, A.; Wermeille, D.; Westerstrom, R.; Gustafson, J.; Felici, R.; Lundgren, E.; Frenken, J. W. M. Surface structure and reactivity of Pd(100) during CO oxidation near ambient pressures. *Phys. Chem. Chem. Phys.* **2011**, *13*, 13167−13171.
(37) Mars, P.; van Krevelen, D. W. Oxidations carried out by means of vanadium oxide catalysts. *Chem. Eng. Sci.* **1954**, *3*, 41−59.
(38) Onderwaater, W. G.; Taranovskyy, A.; Bremmer, G. M.; van Baarle, G. J. C.; Frenken, J. W. M.; Groot, I. M. N. From dull to shiny: A novel set-up for reflectance difference analysis under catalytic conditions. *Rev. Sci. Instrum.* **2017**, *88*, 023704.
(39) Leiden Probe Microscopy B.V., http://www.leidenprobemicroscopy.com/.
(40) van Rijn, R.; Ackermann, M. D.; Balmes, O.; Dufrane, T.; Geluk, A.; Gonzalez, H.; Isern, H.; de Kuyper, E.; Petit, L.; Sole, V. A.; et al. Ultrahigh vacuum/high-pressure flow reactor for surface X-ray diffraction and grazing incidence small angle X-ray scattering studies close to conditions for industrial catalysis. *Rev. Sci. Instrum.* **2010**, *81*, 014101.
(41) Boggio, J. E.; Plumb, R. C. Theory of formation of very thin oxide films on metals. *J. Chem. Phys.* **1966**, *44*, 1081−1086.
(42) Meakin, P. The growth of rough surfaces and interfaces. *Phys. Rep.* **1993**, *235*, 189−289.
(43) McIntyre, J. D. E.; Aspnes, D. E. Differential reflection spectroscopy of very thin surface films. *Surf. Sci.* **1971**, *24*, 417−434.
(44) Nilsson, P. O. Optical properties of PdO in the range 0.5−5.4 eV. *J. Phys. C: Solid State Phys.* **1979**, *12*, 1423−1427.
(45) Yanguas-Gil, A.; Sperling, B. A.; Abelson, J. R. Theory of light scattering from self-affine surfaces: Relationship between surface morphology and effective medium roughness. *Phys. Rev. B: Condens. Matter Mater. Phys.* **2011**, *84*, 085402.
(46) Davies, H. The reflection of electromagnetic waves from a rough surface. *Proceedings of the IEE-Part IV: Institution Monographs* **1954**, *101*, 209−214.
(47) Elson, J. M.; Bennett, H. E.; Bennett, J. M. Scattering from optical surfaces. *Appl. Opt. Opt. Eng.* **1979**, *7*, 191−244.
(48) Aspnes, D. E. Optical response of microscopically rough surfaces. *Phys. Rev. B: Condens. Matter Mater. Phys.* **1990**, *41*, 10334−10343.
(49) Aspnes, D. E. Optical properties of thin films. *Thin Solid Films* **1982**, *89*, 249−262.
(50) Reather, H. *Surface Plasmons*; Springer: Berlin, 1988.
(51) Monine, M.; Pismen, L. M. Roughening of catalytic surface due to reversible surface reconstruction coupled with oscillatory dynamics: a Monte Carlo study. *Catal. Today* **2001**, *70*, 311−320.



DOI: 10.1021/acs.jpcc.7b02054
*J. Phys. Chem. C* 2017, 121, 11407−11415